
Robot-guided Electrophotographic Powder Application System for Powder Bed Fusion of Metals by means of Laser Beam

Julia Förster^{1*}, Maximilian Binder¹, Georg Schlick¹, Christian Seidel^{1,2}, Johannes Schilp^{1,3}

¹Fraunhofer Institute for Casting, Composite and Processing Technology IGCV,
Am Technologiezentrum 10, 86159 Augsburg, Germany

²University of Applied Sciences Munich, Department for Mechatronics and Applied Sciences,
Lothstraße 34, 80335 Munich, Germany

³University of Augsburg, Chair of Digital Manufacturing, Am Technologiezentrum 8,
86159 Augsburg, Germany

*: Corresponding Author 0049 821 90 678 321, julia.foerster@igcv.fraunhofer.de

Abstract

Powder application remains amongst the core challenges in Powder bed based additive manufacturing. Current state of the art does hardly allow processing of powders with low flowability or the processing of multiple materials (multi-material) within one layer. In this paper, a powder application process based on electrophotography is presented to increase the flexibility of additive manufacturing processes using powder bed fusion of metals (PBF-LB/M) as specific reference. A novel conceptual design of an automated 6-axis robot-controlled prototype for electrophotographic powder application in a machine environment are shown. Experiments demonstrate single- and multi-layer powder depositions for the PBF-LB/M typical powder CW106C (CuCrZr1). A first qualitative comparison of the powder application process in the ambient media in atmospheric conditions and in an argon inert gas atmosphere is performed. With the automated powder application, the general inclusion in the PBF-LB/M cycle for multi-layer deposition and melting can be demonstrated.

1. Introduction

With the ambition to process new and different materials in powder bed fusion of metals by means of a laser beam (PBF-LB/M), new application strategies with regard to powder recoating systems are required. Powder application by electrophotography (EP) offers innovative potential. The electrophotographic principle is based on the attraction of electrical charges and has been established in laser printers and photocopiers for decades. This mechanism is considered to be independent of fluidity while providing high local resolution and the high application speed of a laser printer [1].

In this paper, the state of the art first addresses general requirements for powder application in PBF-LB/M as well as current challenges where the electrophotographic process can provide a solution. Since this mechanism is still widely unexplored for PBF-LB/M, the design and development of a prototype is presented. In the concept the specific requirements for the installation of an electrophotographic process in an additive manufacturing machine are addressed with a focus on the precise, robot-guided transport system. The electrophotographic powder application is then tested under machine conditions. Using single-layer deposits under normal atmospheric conditions, the basic process capability and process control are tested within selected parameters. By repeating the powder application, the deposits are stacked and the basic ability to generate a powder bed is investigated. Building on this, the integration of the electrophotographic process into the PBF-LB/M process cycle is demonstrated by recurring melting and powder application for several layers.

2. State of the Art – Powder Application

In powder bed based additive manufacturing, the powder bed properties are directly related to the achievable quality of the components. In PBF-LB/M, not only a homogeneous powder layer, but also a high packing density in the powder bed is beneficial. At the same time, the powder application determines the technological process limits, which must be advanced. In particular, these include:

- a localized powder application according to demand (e.g. limited to the laser exposure area),
- the extension of the powders that can be processed (e.g. low cost powders) and
- the application of multiple powders (multi-material).

Typically used mechanisms for powder application in PBF-LB/M are essentially based on blades, rollers or nozzles and are contact-based. Blade and roller systems always apply powder coatings over the entire surface of the building platform, regardless of the actual component occupancy. Nozzle concepts are suitable for local powder application [2, 3]. They apply the powder mostly as a cluster or linearly at the required locations. What these mechanisms have in common is that they do not allow a flexible change between a full-area and a local, geometrically arbitrary powder application. An economical powder application in line with the flexibility of the powder application would be conceivable through the combination of the mechanisms, which would be associated with increased effort in process control and implementation.

A significant disadvantage of existing powder application systems is that the quality of the powder application depends on the flowability of the powder. Conventional systems are in constant contact with the powder particles during powder application and therefore depend on a high flowability of the powders. The particle shape as well as the particle size distribution (PSD) limit the processable powder spectrum [4, 5]. The production of flowability-optimized powders requires expensive processing and classification of the powder, which makes PBF-LB/M powders cost-intensive [6]. This results in an economic interest in using less expensive powders in the process without causing a loss of quality in the component. Currently, powders with less favorable flow properties are difficult to apply [5].

In the additive multi-material processing an arbitrary and precise application of several powders as well as the separate stocking and supply of the powders is necessary. Grinth et Al. [3] and Schneck et Al. [7] summarize existing procedures and challenges of multi-material processing. The approaches to multi-material manufacturing are based on the adaptation and extension of powder application by combining established application principles. Currently, modifications consisting of two-dimensional and local mechanisms with separate powder reservoirs as well as additional suction units are being tested. Particular challenges arise in the realization of a targeted separation-sharp or graded transition zone of the materials in the coating plane [3, 7]. In addition, there is still the previously described dependence on the flowability of the powders.

The process principle of electrophotography can potentially overcome the mentioned limits of the previous described application mechanisms in one system. As a result, the PBF-LB/M could not only become more economical, but also reach a new technological level.

The contactless, electrostatic particle transport and the use of a photoconductor are decisive for this. The operating principle of a photoconductor as a powder transport medium enables a flexible change between full-area and local powder application. By exposing the photoconductor to light, a geometrically arbitrary, latent charge image is generated on its surface; without this exposure, the powder is applied over the full-area.

Metallic powders present a special circumstance for the physical operating principle due to the material's own electrical conductivity. Some approaches for processing metallic particles show challenges in powder application with the generation of electric fields (E-field) for powder transport. Among other things, the choice of parameters such as electrical potential, polarity or duration of operation can lead to oscillating particles [1] or insufficient particle deposition on the build plate [1, 8]. As a result, single-layer deposition and stacking of particles is impeded. This impairs the construction of a powder bed through multi-layer deposition, which is necessary for

powder bed based fusion of metals. Van der Eijk et al. succeeded in particle transport and stacking of metallic as well as ceramic powders by means of photoconductors under normal atmospheric conditions [9–11]. They demonstrate the basic feasibility of powder application by means of photoconductors through the isolation of the potential-bearing components and targeted process control.

The EP technology has not yet been investigated for the PBF-LB/M process in particular. What remains unexplored is whether the electrophotographic process can operate under machine conditions and in an inert gas atmosphere. In particular, the generation of a sufficiently strong electric field for the powder attraction or powder deposition process can be a challenge, as argon, for example, has only about 75 % of the dielectric strength of air [12]. For PBF-LB/M, however, argon offers the advantage of a low-reaction inert gas atmosphere and therefore minimal influence on the processed materials.

For the sequential investigation of the electrophotographic process with PBF-LB/M-typical, metallic powder, a prototype (EPAMO 1) has already been developed as a translational mechanism for powder deposition by means of an organic photoconductor (OPC). In [13], the basic functionality of the mechanism is demonstrated by single and multiple deposits using spherical steel powder (20MnCr5) with a PSD of 15 – 56 μm under normal atmospheric conditions (air, 20 °C, 25 % rH).

In order to qualify a metal powder application electrophotographic process under machine conditions, it is necessary to develop an optimized and more compact electrophotographic application module (EPAMO 2). The EPAMO 2 is based on the fundamental research findings from the sequential investigations of the process steps for transferring the electrophotographic process to a PBF-LB/M system [13–16].

3. Concept and Development of the EPAMO 2 System

In the development and control of an electrophotographic powder application mechanism, the definition and subdivision of the overall process consisting of (electrophotographic) powder application and powder consolidation by means of a laser beam as well as the selection of suitable components with periphery and process monitoring or control are particularly relevant.

3.1 Subdivision of the Process

An essential aspect of the conception is the definition of the process steps and interfaces (I). Based on conventional electrophotography, the process is divided into 6 process steps. In Fig. 1, these are shown schematically with interfaces. In most cases, the interfaces are formed by measuring points for detecting the process step-dependent surface potential of the photoconductor.

An electric field (similar to a plate capacitor) was used for both powder attraction and powder deposition. For this purpose, the negatively charged photoconductor and the positive powder bed, which was supplied with potential via a high voltage generator (HV), first form an E-field for particle attraction. Similarly, the photoconductor with attracted powder and the potential-supplied negative deposit plate form an E-field for particle deposition.

The electrophotographic powder application begins with the charging of the photoconductor. The target is to apply a homogeneous, temporally constant potential over the area at the photoconductor surface (Φ_{OPC}). Thus, the first interface (I1) is given after charging the photoconductor.

For selective powder attraction, the process phase of imaging takes place. In this process, areas of the OPC are selectively discharged and a latent charge image is created that corresponds to the desired pattern of the subsequent powder layer. After exposure, the surface potential of the photoconductor is reduced by the amount of the exposed, potential-free area and represents the interface (I1*). However, this is left out deliberately for full-area powder attraction.

This is followed by the powder attraction from a powder bed with the interface I2, which reflects the surface potential of the photoconductor with attracted powder ($\Phi_{\text{OPC+Powder}}$). In the developed electrophotographic

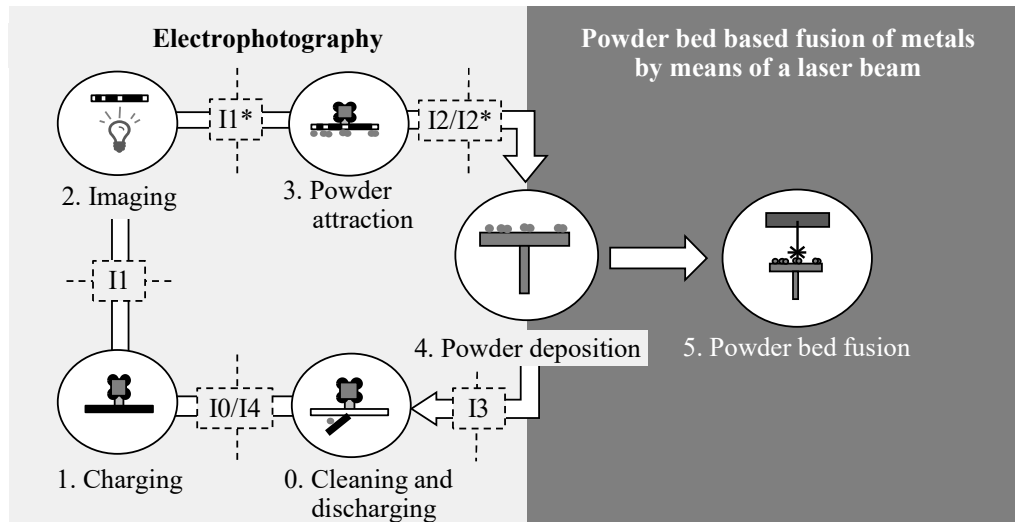


Figure 1: Schematic illustration of the process steps and their interfaces for electrophotographic powder application in connection with powder bed fusion of metals by means of a laser beam.

process, additional charging may be necessary to stabilize the particle potential at the photoconductor, e.g. by means of a corona discharge unit (CU). The subsequent interface is detected with I2*.

Afterwards, powder deposition interface I3 is set up in the electrophotographic process, representing the surface potential of the photoconductor after deposition ($\Phi_{\text{OPC-Powder}}$). The deposition is followed by the cleaning and discharging of the photoconductor as well as the interface I4 or I0, which represent the surface potential on the photoconductor at the end or beginning of the powder application. A recording of I0 directly at the beginning of the powder application serves to monitor possible system disturbances, for example due to interference fields or a malfunction of the sensors. Furthermore, a comparison with I4 could be used to draw conclusions about drift behavior caused by the system. After the powder has been deposited the powder layer has to be solidified by means of the laser beam. At this point, it must be ensured that no process components remain in the laser area and that the laser can act freely on the deposited powder.

3.2. Components, Periphery and Process Control

The SLM 250 HL system from SLM Solutions was chosen to implement the prototype in an additive manufacturing system. During the conceptual design, special attention was on the selection of a suitable transport system for the photoconductor. On the one hand, there are requirements with regard to the available movement and assembly space in the build chamber of around 480 mm x 420 mm x 380 mm and the ambient temperatures of up to 60 °C [17] as well as to metal powder and welding smoke. On the other hand, it is important to integrate the process components and to reach every station with the photoconductor. A precise, three-dimensionally operating system with a linear travel deviation of maximum 0.1 mm has been specified for guiding the photoconductor over the individual components. In analogy to a plate capacitor, where the distance between the plates forming the field has a linear effect on the E-field [13], it is assumed that even a deviation of 0.1 mm leads to a change in the electric field of around 10 %. A 6-axis vertical articulated robot arm of the type MECA500 from Mecademics was selected based on the given requirements. As part of the selection process, a verification of the linear movement accuracy has been carried out. The measurement setup and the results of the linear movement in the plane are summarized in Fig. 2.

The selected travel motion simulates the accuracy of moving the photoconductor over components mounted on the floor of the build chamber. The measuring accuracies are indicated in brackets in the legend of the diagram behind the respective measuring devices. Even with the slight exceeding of a measured value in the chosen setup (measuring device 2, at 20 mm) it is assumed that the specified accuracy limit can be met with the MECA500.

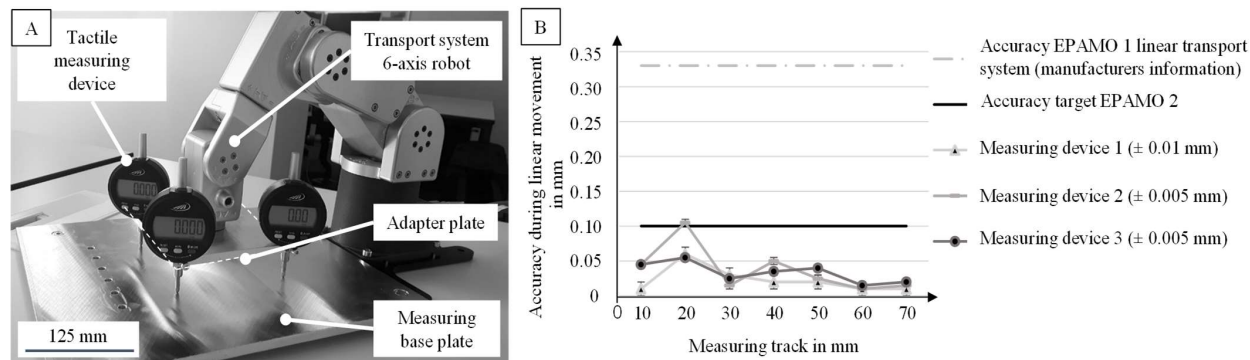


Figure 2: Verification of the accuracy of the MECA500 during linear movement
 A: Measurement setup on the MECA500 with three dial instruments, B: Diagram of the measurement results.

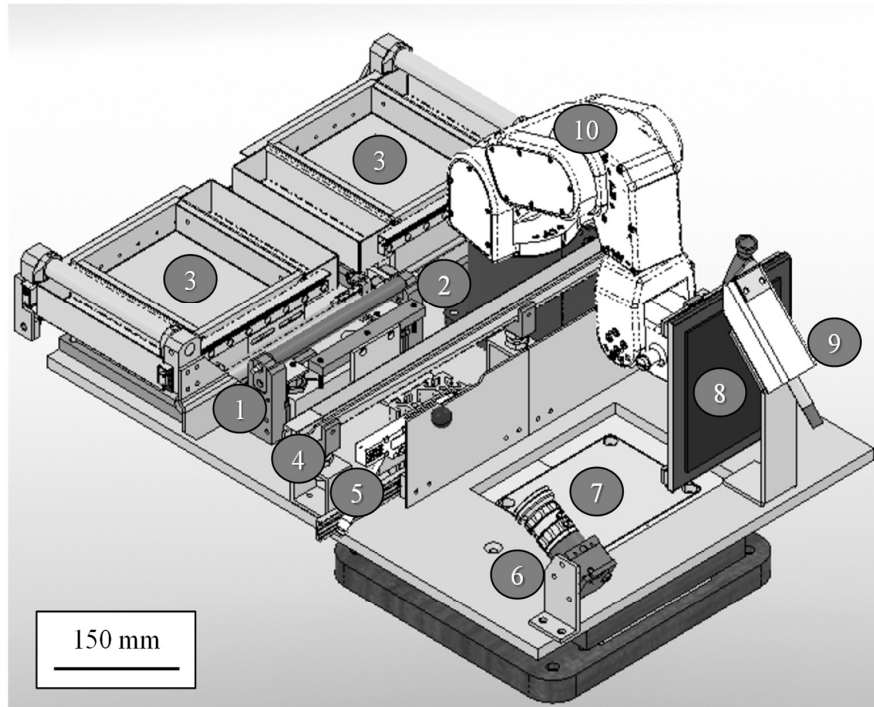
The resulting concept including the transport system and the process-relevant components is shown in Fig. 3. For the electrophotographic process, it is essential that the voltage-carrying components are insulated from the rest of the system and that no charge carriers can flow away. Therefore, the voltage-carrying components of positions 1, 3, 4, 7 and 8 are located on insulating polymer plates. The photoconductor electrode is insulated directly on the robot holder. These components are each connected to the HV generator of the type iseg HV SHR 4060 and can be controlled individually in terms of polarity and potential level.

For the exposure and the associated generation of latent charge patterns on the photoconductor or the selective attraction of powder, three laser diodes are positioned under pos. 2. The generation of charge patterns is achieved by the movement of the photoconductor.

Since manual operation of the process is not possible in an inert gas atmosphere, automatic powder supply and automatic cleaning of the photoconductor after powder deposition are necessary for running the EPAMO 2 in a machine environment. Special attention is therefore paid to the powder supply stations (Fig. 3, Pos. 3). Each powder reservoir is equipped with an automatic smoothing unit, which automatically prepares and flattens the powder bed surface after attraction. To remove the residual powder from the photoconductor, a gas stream is directed at the photoconductor through a cylindrical nozzle with a diameter of approx. 10 mm. The nozzle is located in an enclosure with a square opening along which the photoconductor is guided for cleaning (Fig. 3, item 9). The gas stream containing residual powder is extracted above the opening to minimize contamination of the installation space.

The photoconductor is an organic photoconductor of the type OP-3CL from Brother, which is commercially available as a belt. In order to transfer the previous findings with EPAMO 1, a photoconductor area of 50 mm x 50 mm was used for experimentation of the system. The process can be equipped with a maximum photoconductor area of 150 mm x 120 mm, which is adapted to the geometric machine conditions. To minimize the undesired effects of fringing fields and inhomogeneous field forces during powder attraction, the dimensions of the powder beds are 120 mm x 100 mm, which is smaller than the maximum photoconductor area. The dimensions of the construction plate of 120 mm x 100 mm are matched to the area of the attractable powder surface.

To detect the surface potential on the photoconductor at the interfaces of the process steps (see Fig. 1), a measurement of the potential on the principle of a field mill is selected. On the one hand, the principle enables a contact free measurement, which is necessary due to adhering particles, and on the other hand, it does not extract any energy from the system during the measurement, so that the measurement result is not biased. A Keyence SK-050 sensor is used to measure the potential with a tolerance of ± 10 V. The support system guides the photoconductor over the sensor in the near-field measuring range (16 mm) at the respective measuring points. Thus, measured values can be recorded for 10 to 14.



- | | | |
|--------------------|-------------------------|---|
| 1: Charging roller | 5: Electrostatic sensor | 8: Photoconductor with attracted powder |
| 2: Imaging unit | 6: Camera | |
| 3: Powder bed | 7: Deposition plate | 9: Cleaning and discharging unit |
| 4: Corona unit | | 10: Robot transport system |

Figure 3: Concept model of the robot-guided, electrophotographic powder application module (EPAMO 2) for system integration in a SLM 250 HL.

4. Electrophotographic Powder Application under Processing Conditions

Focus of the investigations is to evaluate the functionality of the electrophotographic powder application and to integrate it into PBF-LB/M. The interplay between the powder application and the powder solidification was also considered. It is important to evaluate the stackability of the powder layers on top of each other by repeating the application process. The essential difference in the process sequence is that in the case of single deposits, the powder layer is removed after each deposit and evaluation; when stacking the layers, the previous layers remain on the build plate. After the experimental procedure for stacking single-layers to form an optically dense powder bed under argon atmosphere, the melting of a geometry in the powder bed and, in particular, the continuation of the powder application took place. The powder layers were stacked again, but on the partially solidified material. In the following, the experimental approach is described first. For this purpose, relevant preliminary investigations are presented. Subsequently, the results of the powder application under ambient conditions are presented and discussed. In this paper the selective attraction or deposition is not considered in the investigations of the functionality under machine environmental conditions. The possibility of charging the photoconductor in an argon atmosphere was demonstrated by [14]. The exposure of the photoconductor and selective powder attraction are described in [16].

4.1 *Experimental Approach and Preliminary Investigations*

In the following experiments and in analogy to EPAMO 1 the powder was deposited on an aluminum plate. For higher contrast on the deposition plate, spherical 1.7147 (20MnCr5) and CW106C (CuCrZr1) powder with a PSD of 15 – 56 μm were chosen.

The powder application is evaluated qualitatively with a visual observation based on photographic images of the powder deposits and a classification into categories based on the following criteria:

- Full-area particle coverage: The powder deposit corresponds to the maximum photoconductor area,
- Density of particle coverage: The area covered with particles is visually recognizable on the deposition plate,
- Homogeneity: The particle coverage of the deposit appears uniform.

The derived categories are summarized in Table 1.

Table 1: Categories for the qualitative evaluation of powder deposits

Category	Description
A	Full-area, homogeneous and optically dense layer
B	Partial-area but optically dense, homogeneous layer
C	Full-area, homogeneous, not dense layer
D	Partial-area, optically non-homogeneous and not dense layer
E	No layer visible

Preliminary experiments showed that a deposit that is not full-area but appears visually dense and homogeneous (category B) can be increased in area and density to a category A by stacking the layers. However, a full-area, non-dense or inhomogeneous layer – also by increasing the potentials – was found hardly or not stackable at all. These layers are assigned to categories C and D.

The Fig. 4 shows exemplary deposits with the categories achieved in the experiments in atmospheric conditions. As can be seen from the example for category C, irregularities appeared, for example, in the form of a clear edge formation in connection with a lack of particle occupation within the surface as well as x-shaped particle concentrations. It is assumed that these phenomena are associated with an excessively high electric field between the particle-covered OPC's surface and the deposit plate and are concentrated at the respective areas. Which effects led to these patterns cannot be clearly explained so far. Geometric influences on the formation and concentration of the field lines are suspected – for example, from edge effects or peak discharges on the OPC carrier or the deposit plate. This hypothesis is congruent with the observed lack of stackability of the deposits, since in this case the electric field cannot be used homogeneously over the surface for the powder deposit and thus no homogeneously distributed powder deposit would be achievable. Category E powder deposits are considered to occur due to artefacts or a significantly too low E-field. In this case, the potentials on the components must be increased.

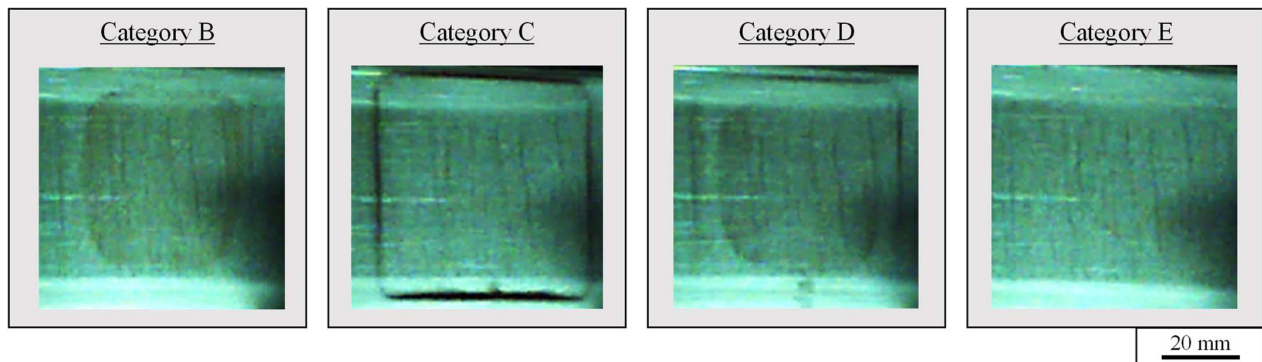


Figure 4: Representation of exemplary images of the powder deposits with classification into the corresponding categories of the qualitative evaluation.

The best powder deposits with CW106C under atmospheric conditions for EPAMO 2 was achieved in category B with the process parameters shown in Table 2.

Table 2: Process parameters and relevant potential measurements of the interfaces for generating the powder deposits in category B with CW106C under atmospheric conditions (20 °C, 25 % rH).

Process parameter	Value	Description
Φ_{OPC} (I1)	-250 ± 25 V	Measurement surface potential of the OPC after charging
P_{PB}	1,200 V	Potential of the powder bed
$\Phi_{OPC+Powder}$ (I2)	336 ± 31 V	Measurement surface potential of the OPC after powder attraction
E_{ATT}	1.81 MV/m	Calculated approximation of the E-field for attraction
P_{CU}	1,200 V	Potential of the corona unit
$\Phi_{OPC+Powder+CU}$ (I2*)	278 ± 30 V	Measurement surface potential of the OPC with attracted powder after corona unit
P_{DP}	-175 V	Potential of the deposit plate
$\Phi_{OPC-Powder}$ (I3)	-24 ± 14 V	Measurement surface potential of the OPC after powder deposition
E_{DEP}	0.56 MV/m	Calculated approximation of the E-field for deposition

The measurement of the surface potentials at the interfaces of the process phases is used for process control and can provide information about possible changes in the process and serve to estimate the E-fields. The E-field of attraction (E_{ATT}) or deposition (E_{DEP}) can be estimated in analogy to a plate capacitor in a preliminary approximation via the formulas Eq. 1 or Eq. 2 [13].

$$\text{Eq. (1)} \quad E_{ATT} = \frac{P_{PB} + |\Phi_{OPC}|}{d_{ATT}} \quad \text{Eq. (2)} \quad E_{DEP} = \frac{\Phi_{OPC+Powder+CU} + |P_{DP}|}{d_{DEP}}$$

The distances for powder attraction (OPC – powder bed, d_{ATT}) and deposition (OPC with attracted powder – deposition plate, d_{DEP}) were not changed and kept constant at 0.8 mm. For the preliminary experiments, the automatic lifting of the powder bed was left out, which meant that the height of the powder bed remained constant at 10 mm. The powder bed surface was manually filled after each attraction and automatically flattened by means of the smoothing unit. The surface potential of the OPC was applied in the charging step by contact to a potential charging roller and repeated until the desired potential was reached with a predefined tolerance of ± 25 V. With a powder bed potential of 1,200 V, full-area powder attraction could be reproducibly achieved. At higher potentials, flashovers between the powder bed and the OPC occurred more frequently, causing a sudden potential equalization and causing the powder application process came to a standstill.

The deposition quality for single-layers does not exceed category B. This is an indication that the system and the process window are not yet optimally matched. It is assumed that there are effects and parameters in the system that are hierarchically superior to the process control parameters (of distances and potentials). Thus, a possible influence of components, such as the photoconductor or the deposition plate material, on the powder application process is the subject of future research and further system optimization.

4.2 Experiments with Electrophotographic Powder Deposition in an Argon Atmosphere and Integration into the Laser Beam Melting Process

Based on the preliminary investigations, powder deposits were carried out in an atmosphere of argon with a residual oxygen content of less than 0.5 %. The distances d_{ATT} and d_{DEP} were kept constant at 0.8 mm for single

and multi-layer deposits. The powder was prepared by the automatic smoothing system of the powder bed. Fig. 5 shows an example of the powder deposits of a single and subsequent multi-layer deposits. This shows for the first time that electrophotographic powder deposition works in an argon atmosphere and that it is fundamentally possible to build up a powder bed.

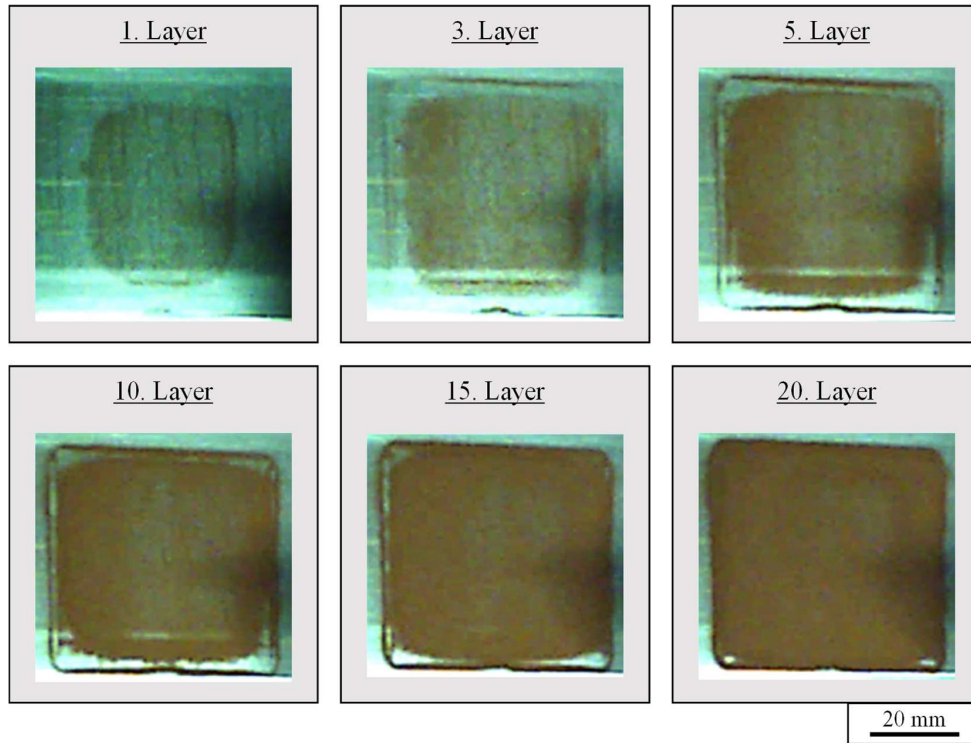


Figure 5: Build-up of an optically dense powder bed of CW106C by electrophotographic multi-layer deposition in an argon atmosphere.

Based on the single-layer deposition (1 layer), it can be seen that the deposition quality also corresponds to category B in this experimental series. With increasing powder deposits, the coverage area is enlarged and compacted, so that from approx. 5 layers onwards a optically dense powder layer is clearly recognizable. With multi-layer deposits of more than 20 layers, there is a risk – without adjusting the distance to the deposit – of sudden powder dislocations due to an excessively large E-field caused by the growing layer.

Table 3 summarizes and compares the associated process control parameters as well as the relevant measured potentials of the process interfaces to the single-layer deposits of category B in argon as well as to the known values of the deposits in atmospheric conditions. The process parameters were kept constant for the multi-layer deposits. The I-values I1, I2 and I2* of the powder attraction did not change. Only the value I3 is directly related to the powder deposits and became increasingly negative as the number of layers increased (constant d_{DEP}).

The values of the potentials for controlling the process and the measured values of the surface potentials of the interfaces are lower in comparison with argon and the preliminary experiments in atmospheric conditions. The OPC potential is also predefined here and is therefore similar to the potential in atmospheric conditions; the potential of the corona unit was constant.

In the column "Ratio argon to air" the argon values are shown in relation to the values under atmospheric conditions to quantify the comparison as a percentage.

Table 3: Process parameters for the generation of a single-layer category B powder deposit with CW106C under argon atmosphere in comparison to atmospheric conditions.

Process parameter	Value argon	Value air (20 °C, 25 % rH)	Ratio argon to air
Φ_{OPC} (I1)	-250 ± 25 V	-250 ± 25 V	-
P_{PB}	850 V	1,200 V	71 %
E_{ATT}	1.38 MV/m	1.81 MV/m	76 %
$\Phi_{\text{OPC+Powder}}$ (I2)	41 ± 12 V	336 ± 31 V	12 %
P_{DEE}	1,200 V	1,200 V	-
$\Phi_{\text{OPC+Powder+CU}}$ (I2*)	38 ± 11 V	278 ± 30 V	14 %
P_{DP}	-175 V	-175 V	-
E_{DEP}	0.27 MV/m	0,64 MV/m	42 %
$\Phi_{\text{OPC-Powder}}$ (I3)	-14 ± 5 V	-24 ± 14 V	58 %

The maximum powder bed potential under argon was reached at approx. 850 V (at around 71 % of the air value). As a result, the nominal E-field for attraction was also comparably lower (around 76 %). A possible connection may exist with the reduced dielectric strength of argon. This would be congruent with the observed flashovers already at 850 V at the powder bed. The interface values of I2 and I2*, which reflect the potential of the OPC with attracted powder, are perceptible both values for argon are below the values achieved in atmospheric conditions. The measured potential values depend proportionally on the potential on the powder bed (P_{PB}). With increasing the potential on the powder bed, the values of the directly following interfaces increase. It can be assumed that further effects influence the measured values resulting from the attraction step. Conceivable effects would be the electrodynamic interaction of the metallic particles in the collective, the resulting dielectric behavior of a metal powder depending on the atmosphere or the actual height of the powder bed.

The potential at the deposition plate is set at -175 V in both atmospheres. Due to the reduced potential at the photoconductor after powder attraction (I2*), the approximated E-field for the deposit is also lower. In argon, this value is less negative for a deposit of quality B (around -14 V). Due to these values, it is not yet possible to make a generally valid statement about process control purely on the basis of the detected surface potentials of the interfaces. Preliminary experiments showed a dependence of the potential at the photoconductor after deposition (I3) on the deposit quality. This, in conjunction with the not yet optimal deposition quality that can be achieved so far, indicates that the powder deposition process requires further investigation.

Continuing the investigation into the generation of electrophotographic powder deposits in an argon atmosphere, the integration into PBF-LB/M and in particular the deposition on melted material is to be tested. A square of 10 mm x 10 mm of this layer was solidified with the laser. The tested laser parameters are listed in table 4. The parameters have been chosen following Anstaett for melting CW106C in a SLM 250 HL machine [18].

Table 4: Laser parameters used for powder solidification of CW106C in an SLM 250 HL.

Laser parameter		Powder specification	
Laser power	400 W	Material	CW106C
Hatch spacing	0.125 mm	Particle size distribution	15 – 56 μm
Scan speed	600 mm/s	Particle shape	spherical

Measurements of the layer thickness from preliminary investigations showed a value of around $64\ \mu\text{m}$ for a 4-layer deposition [13]. Assuming this layer height for CW106C as well with a reduction of the layer due to the melting of the particles of about 50 % [19], the melted layer height is approximated about $30\ \mu\text{m}$. After melting, the build plate is lowered by $30\ \mu\text{m}$ and the deposition process continues. The process was continued until the melted surface is optically densely covered with powder.

Fig. 6 shows an example of powder application for multi-layer powder deposits with subsequent solidification of the powder. After 5 layers, the powder deposit seems to be optically dense and an almost square-shaped area could be melted. The melted surface appears partly out of focus in the edge areas and does not correspond to the idealized target geometry there. This observation could be a result of dislocated powder particles due to the inert gas flow during the fusion process.

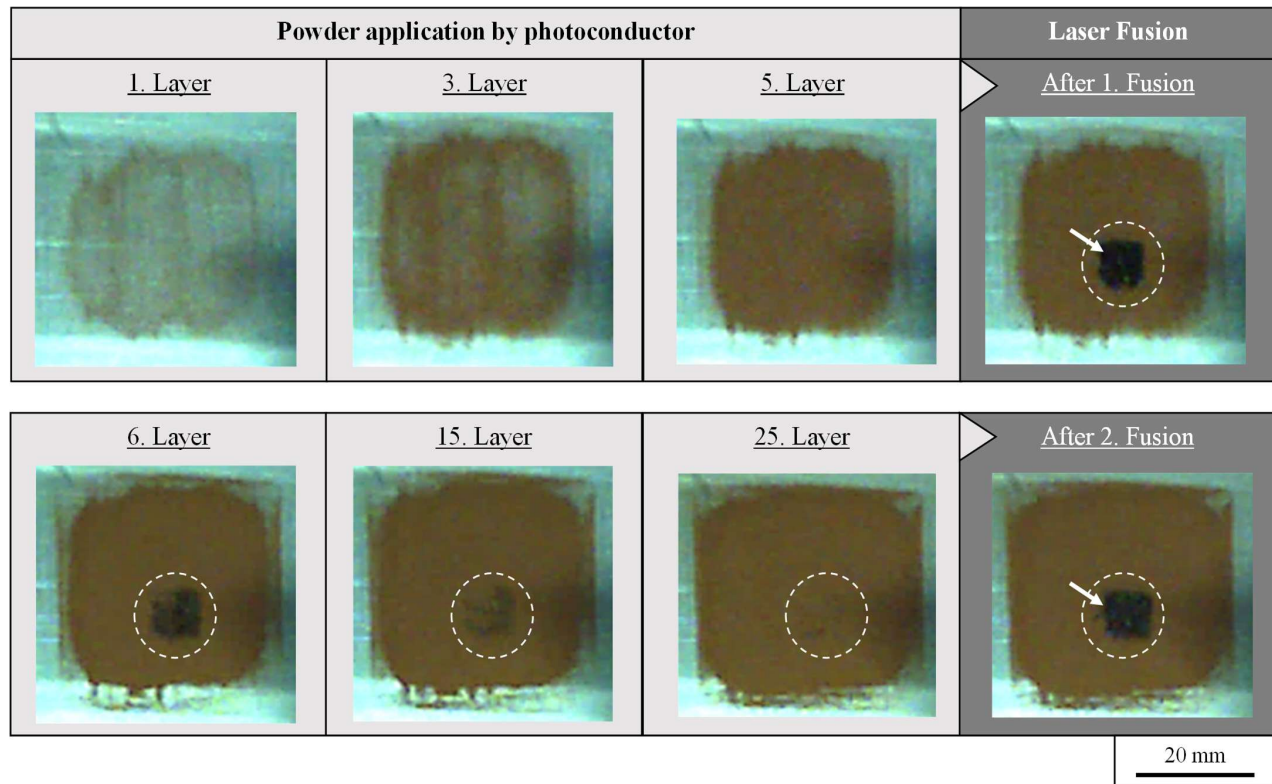


Figure 6: Powder application by means of photoconductor in argon atmosphere and solidification in the process cycle.

By continuing the powder application, it can be shown that the melted area is covered with powder. Further the powder application not only deposits powder on the melted area, but also extends the maximum deposition area and increases the optical density. This means that the electrophotographic powder application is in general suitable for generating a powder bed in a PBF-LB/M process.

The appearance that more layers are needed to cover the melted area than when depositing without the prior melting can be a result of the non-optimal process window in the process control. One possible reason for this could be related to the current gap between the OPC and the resulting height of the deposits so far. Within this experiments the actual height of the deposited powder layers cannot be detected with the qualitative evaluation. With the lowering of the build plate, the distance between the OPC and the deposit plate becomes undefined, so that the determined potentials are no longer sufficient to generate deposits of higher categories. The distance is as mandatory for the electrophotographic process and the E-field as the potentials. In the future, this challenge could be optimized by e.g. an optical distance measurement.

With the parameters used for melting the layers, it was not possible to achieve a continuous material connection of the CW106 on the aluminum build plate, so no metallographic examination of the melted material was carried out. In future, experiments should be performed with the powder and the building plate paired in the same material.

5. Conclusion and Outlook

The investigations in this paper build on existing work into electrophotographic powder deposition with 1.7147 (20MnCr5) under atmospheric conditions. A precise robot-guided system has been designed and developed for the investigation in argon atmosphere and the integration into a machine for powder bed fusion of metals with a laser beam. With the use of a photoconductor in conjunction with electrostatic powder application, it is possible to apply powder as required, independent of the powder's flowability. In addition with the design of the EPAMO 2 to supply the powders, multiple powders can be applied in one process.

But utilizing copper alloy CW106C (CuCrZr1), it was shown in single and multi-layer deposits that other metal powders can also be applied using electrophotography. In the determined process window, a transfer of the process to an argon atmosphere has been achieved for the first time. Based on this, the integration of the process into powder bed fusion was demonstrated. Optically dense multi-layer deposits have been melted and the filling of the powder bed could be continued with the deposition process. The deposition quality is to be further stabilized and optimized in the future. It can be shown that the electrophotographic powder deposition system has the potential to satisfy the requirements of a deposition system for PBF-LB/M and at the same time push the technological process limits.

Acknowledgements

The authors express their sincere thanks to the State of Bavaria and its Bavarian Ministry of Economic Affairs, Regional Development and Energy StMWi for funding the project Multi-material Center Augsburg.

References

- [1] Kumar, A. V.; Dutta, A.; Fay J. E.: Electrophotographic printing of part and binder powders. *Rapid Prototyping Journal* Vol. 10 (2004), p. 7–13.
- [2] Ott, M.; Zaeh, M. F.: Multi-Material Processing in Additive Manufacturing. In: 21st Proceedings of the Solid Freeform Fabrication Symposium, (2010), p. 195–203.
- [3] Girnth, S.; Koopmann, J.; Klawitter, G. et al.: 3D hybrid-material processing in selective laser melting: implementation of a selective coating system. *Progress in Additive Manufacturing* 4 (2019), p. 399–409.
- [4] Spierings, A. B.; Voegtlin, M.; Bauer, T. et al.: Powder flowability characterisation methodology for powder-bed-based metal additive manufacturing. *Progress in Additive Manufacturing* 1 (2016), p. 9–20.
- [5] Vock, S.; Klöden, B.; Kirchner, A. et al.: Powders for Powder Bed Fusion: A Review. *Progress in Additive Manufacturing* (2019).
- [6] Schleifenbaum, J. H.; Tenbrock, C.; Emmelmann, C. et al.: Future AM. In: Neugebauer, R. (Hrsg.): *Biologische Transformation. Futur AM*, Berlin, Heidelberg: Springer Berlin Heidelberg (2019), p. 229–250.
- [7] Schneck, M.; Horn, M.; Schmitt, M. et al.: Review on Additive Hybrid- and Multi-Material-Manufacturing of Metals by Powder Bed Fusion – State of Technology and Development Potential. *Progress in Additive Manufacturing* (2020).
- [8] Kumar, A. V.; Dutta, A.: Investigation of an electrophotography based rapid prototyping technology. *Rapid Prototyping Journal* 9 (2003), p. 95–103.
- [9] Boivie, K.; Karlsen, R.; Van der Eijk, C.: Material Issues of the Metal Printing Process, *MPP* (2006), p. 197–208.
- [10] Boivie, K.; Karlsen, R.; Van der Eijk, C. et al: Issues of Incremental Graded Metallic Materials by the Metal Printing Process, *MPP. Additive Layered Manufacturing From Evolution to Revolution* (2008).
- [11] Boivie, K.; Karlsen, R.; Åsebø, O.: The Metal Printing Process; The Development of a New Additive Manufacturing Process for Metallic Materials. *Swedish Production Symposium* (2008).
- [12] Lehr, J.; Ron, P.: *Foundations of Pulsed Power Technology. Electrical Breakdown in Gases*. Hoboken, NJ, USA: Wiley (2017).
- [13] Foerster, J.; Vranjes, K.; Binder, M. et al.: Electrophotographic Powder Application for Metal Powder bed based Additive Manufacturing. *Cirp Conference in Electro Physical and Chemical Machining* (2022).

- [14] Foerster, J.; Michatz, M.; Anstaett, C. et al.: Aspects of Developing a Powder Application Module based on Electrophotography for Additive Powder Bed based Processes. *Machining Innovations Conference for Aerospace Industry* (2020), p. 147–152.
- [15] Kindermann, P.; Michatz, M., Foerster, J. et al.: Technological Potential of Electrostatics for Powder Bed Fusion Processes. *EuroPM Congress&Exhibition* (2019).
- [16] Foerster, J.; Michatz, M.; Binder, M. et al.: Electrostatic powder attraction for the development of a novel recoating system for metal powder bed-based additive manufacturing. *Journal of Electrostatics* (2021).
- [17] Binder, M.; Dirnhofer, C.; Kindermann, P. et al.: Procedure and Validation of the Implementation of Automated Sensor Integration Kinematics in an LPBF System. *53rd CIRP Conference on Manufacturing Systems* (2019).
- [18] Anstaett, C.; Seidel, C.; Reinhart, G.: Multi-Material Fabrication of Copper-Chrome-Zirconia and Tool Steel 1.2709 by Powder Bed Based Laser Beam Melting. *Fraunhofer Direct Digital Manufacturing Conference* (2018).
- [19] Spierings, A. B.; Levy, G.: Comparison of density of stainless steel 316L parts produced with selective laser melting using different powder grades. *SFF-Symposium* (2009).